

Article

Tracking the Role of Policies and Economic Factors in Driving the Forest Change Trajectories within the Guangdong-Hongkong-Macao Region of China: A Remote Sensing Perspective

Yuyang Xian ¹, Yongquan Lu ¹, Zipporah Musyimi ² and Guilin Liu ^{1,*} 

¹ School of Geography, South China Normal University, Guangzhou 510631, China; xianyuyang@m.scnu.edu.cn (Y.X.); lyq98@m.scnu.edu.cn (Y.L.)

² Department of Environmental Remote Sensing and Geoinformatics, University of Trier, 54286 Trier, Germany; s6zimusy@uni-trier.de

* Correspondence: liuguilin@m.scnu.edu.cn or guilinsiwo@163.com

Abstract: Though forest ecosystems play a critical role in enhancing ecological, environmental, economic, and societal sustainability, on a global scale, their future outlooks are uncertain given the wide-ranging threats they are exposed to. The uniqueness of this study is to provide a line of evidence in which forest change trajectories are not only tracked but also evaluated through the lenses of forestry and economic oriented events' timelines. The dynamics of forest change trajectories were mined using a temporal model. To understand the forces driving the changes, the change trajectories were linked to the timelines when forestry policies and economic factors were adopted. During 1980–1990, the forest change trajectory assumed a peak (forest gain). This was interpreted as a response to the adoption of policies that promoted ecological conservation. During 1995–2010, the forest change trajectories reflected the response to the antagonistic effects of forest-oriented policies and the economy-oriented drivers. During 2010–2015, the forest change trajectories assumed a deep (forest loss). This was attributed as a response to the economy-oriented factors. However, inferences from the results indicated that deforestation driven by economic factors was restricted by forest management policies. Though the role of economic factors has promoted developments within the study area, forest policies still constrain illegal logging and play a key role in protecting forests. We hope that insights from this study will inform, support and guide decisions for precise and smart sustainable forest management plans.

Keywords: forest change trajectories; spatial-temporal analysis; remote sensing; forest policy and economic factors; Guangdong-Hongkong-Macao (GHKM)



Citation: Xian, Y.; Lu, Y.; Musyimi, Z.; Liu, G. Tracking the Role of Policies and Economic Factors in Driving the Forest Change Trajectories within the Guangdong-Hongkong-Macao Region of China: A Remote Sensing Perspective. *Land* **2021**, *10*, 87. <https://doi.org/10.3390/land10010087>

Received: 14 December 2020

Accepted: 13 January 2021

Published: 18 January 2021

Publisher's Note: MDPI stays neutral with regard to jurisdictional claims in published maps and institutional affiliations.



Copyright: © 2021 by the authors. Licensee MDPI, Basel, Switzerland. This article is an open access article distributed under the terms and conditions of the Creative Commons Attribution (CC BY) license (<https://creativecommons.org/licenses/by/4.0/>).

1. Introduction

Forest plays a critical role in the provision of many ecosystem services, according to the Millennium Ecosystem Assessment (MEA) [1]. For example, they provide supporting services (nutrient cycling, seed dispersal, and soil conversation), provisioning services (timber, fuelwood, and food stuff), cultural services (source of aesthetic recreational, and spiritual values) and regulating services (water shed protection, biodiversity protection, and climate change mitigation) [2,3]. On a global scale, however, their functional integrity continues to be, undervalued, interfered, disturbed, and compromised [1,4]. This implies that their resilience is exposed to a range of vulnerabilities and threats and, hence, their future outlooks are uncertain. The concern is much more prevalent in developing economies where, due to booming populations, industrialization, and urban agglomerations, forests are cleared to meet the demand for space [5]. Even if the whole forest is not cleared, fragmenting the forest ecosystem alters its natural structure. The forest fragments act as blocks that break the holistic flow of the ecosystem services that promote environmental, economic, and social

well-being. This underlines why information on forest dynamics and their driving forces is key input to understanding the role of anthropogenic activities on ecosystem services [5].

Land use/cover change (LUCC) can directly reflect the forest change amplitude, direction and trend. The reported approaches on LUCC include field observation, meta-analysis [6–8] and remote sensing (RS) [9]. The rapid development in RS technology has opened new possibilities to effectively monitor forest cover changes in terms of time, costs, and logistics. The availability of cost-free satellite data archives of dense time series observations to the public domain has made forest monitoring remarkably cost effective. RS images data cover expansive areas including remote areas that would otherwise be too difficult to reach during field observations making the logistics of forest monitoring remarkably effective. RS images from platforms such as NOAA/AVHRR [10,11], MODIS [12–15], and Landsat [16,17] are commonly have been widely used to analyze forest cover dynamics in space and time.

LUCC can be detected from RS products using bi-temporal detection and time trajectory analysis [18]. The bi-temporal detection approaches use data of two different epochs to reveal the changes. Time trajectory analysis, on the other hand, captures detailed LUCC dynamics that reveal the trajectories over time [19]. Owing to the detailed nature in which temporal trajectory analysis can reveal the changes, the approach has, in the past, been used to reveal deforestation and forest fragmentation within the Amazon [20,21], land cover changes in arid zones in the face of climate change [22], tropical forest disturbance [23], forest cover changes in southern Chile [24] and arable land changes in an economically viable location in China [25]. In most of these studies, derivatives from satellite images such as indexes are commonly used as proxies for green land cover. The most widely used indexes include the Normalized Differential Vegetation Index (NDVI) [26], Enhanced Vegetation Index (EVI) [27] and Normalized Difference Fraction Index (NDFI) [28] as well as other indices related to the forest growth such as Normalized Combustion Rate (NBR) [29]. In many of the past studies, inferences to indicate the health of the forests are linked to climatic conditions. Rarely are these inferences analyzed to indicate the synergistic and antagonistic role of forest management policies as well as economic factors on forest change dynamics.

The Guangdong-Hongkong-Macao (GHKM) region is particularly relevant for this study because it represents management conflict hot spot where stakeholders' interests clash owing to the land potential and its intrinsic value. Ecologically, the region is an important forestry resource bank with a host of species. On the other hand, the region has exceedingly high economic potential in China and thus is on high demand for investors. Therefore, the development of sustainable plans is conflicted by entities promoting economic development agendas against the interests of those campaigning for forest protection and ecological conservation [30]. This scenario though locally unique to this region, it is relatable to many regions of the world where conflicts of interest have seen irreversible conversion of expansive forested areas to other land uses. As such, we use it as a case study with the hope that the insights from this research can inform a global audience.

Our research takes a three-fold approach: First, the spatiotemporal dynamics of forested areas in GHKM are analyzed by constructing temporal trajectories. The second phase involves linking the change trajectories to the timelines of forestry policies and economic factors were adopted to reveal the transformation from forest policy-oriented forest change drivers during 1980–1990 to economy-oriented drivers during 2010–2015. In the third phase, deforestation is linked to physical factors (such as slope and altitude) to evaluate the constraint role of policies when economic factors are the lead actors. Specifically, this paper aims to (1) track spatial and temporal dynamics of forest patterns in GHKM during 1980–2015; (2) elaborate the synergistic role of forest policy and economic drivers in forest change dynamics and trajectories.

2. Materials and Methods

2.1. Study Area

The “Guangdong-Hongkong-Macao” region (GHKM) in China is located within the southern coastal zone covering three provinces including; Guangdong, Hong Kong and Macao (Figure 1). GHKM is characterized by a subtropical humid and warm monsoon climate. As such, the region is heavily endorsed with expansive forestry resource of high species richness, such as mangroves, rubber, tropical fruit trees, bamboos, and tea trees. To better capture the forest features and rightly articulate their change patterns and dynamics, this study divides the GHKM region into four: the Eastern Guangdong region (EGR), the Western Guangdong region (WGR), the Northeast Guangdong region (NGR) and the Guangdong-Hong Kong-Macao Greater Bay Area (GHKM-GBA) [31]. The EGR region is a famous tea production zone and covers four cities namely: Chaozhou, Shantou, Shanwei and Jieyang. The WGR region is well known for agricultural production especially tropical fruits in Leizhou Peninsula and covers three cities including Maoming, Zhanjiang and Yangjiang. The NGR is a mountain zone and has the highest altitude in the GHKM and includes Shaoguan, Qingyuan, Meizhou, Heyuan and Yunfu city. The GHKM-GBA is among one of the highly developed urban agglomeration in China and includes Guangzhou, Shenzhen, Zhuhai, Foshan, Huizhou, Dongguan, Zhongshan, Jiangmen, Zhaoqing, Hong Kong and Macao City.

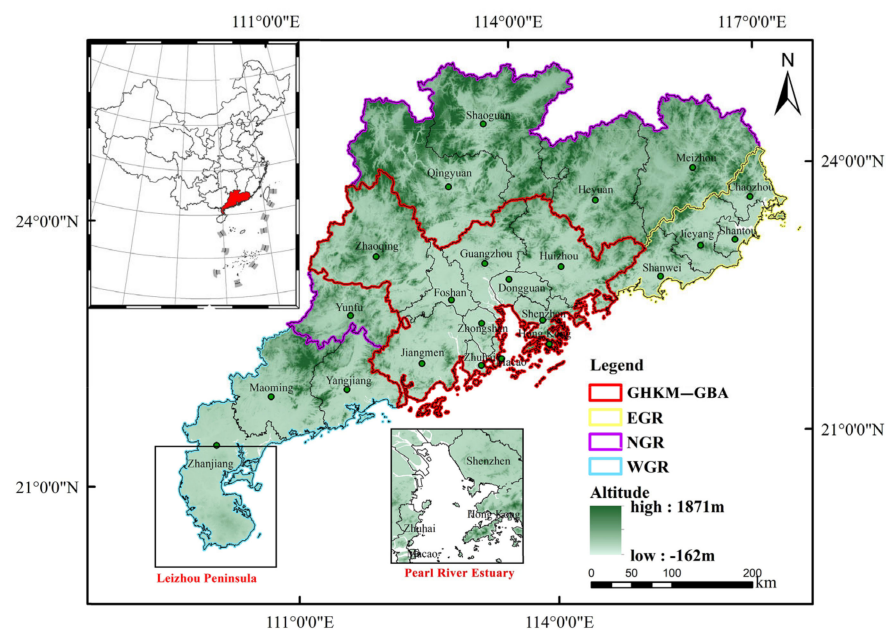


Figure 1. Location of the study area in China illustrating the four regions of the study.

2.2. Data

The gridded land use data from 1980 to 2015 and vector data of administrative divisions was obtained from Data Center for Resources and Environmental Sciences, Chinese Academy of Sciences (RESDC) (<http://www.resdc.cn>) [32]. The land use data was generated from Landsat data remote sensing images, with reference to China’s land-use remote sensing mapping system [32]. The forest types were categorized into: closed-canopy forests (canopy closure > 30%), shrub (canopy closure > 40% and height below 2 m), sparse forests (with canopy closure between 10 and 30%), and other-forest types (e.g., orchards) [33]. The accuracy of the forest type’s classification was greater than 90% for the 1980 data [34], 95% for the 1990–2000 data [35], 98% for the 2005 data [36], 94.3% for 2010 data [37] and 93% for the 2015 data [38]. The forest policies were acquired from the central government of China, China forestry network and from Guangdong Provincial People’s Government websites. The forestry output values, GDP per capita and agricultural

labors data after 1990 was obtained from the statistical yearbook of Guangdong province. The physical data of the study area such as altitude and slope data were derived from the CGIAR-CSI SRTM/SRTM 90 m DEM Digital Elevation Database (<http://srtm.csi.cgiar.org>).

2.3. Methods

To construct a temporal trajectory model for the estimation of the forest dynamics (Figure 2), the land use data from 1980 to 2015 was classified into forest/non-forest maps. 50 temporal trajectories were selected and summarized into five categories namely:

- Permanent forest: A forest pixel that without change in status remained a forest pixel between 1980 and 2015.
- Permanent non-forest: A non-forest pixel that remained non-forest between 1980 and 2015 without change in status.
- Afforestation: A pixel that was non-forested in the early period but later transformed into a forested pixel within four temporal trajectories.
- Deforestation: A forested pixel that was transformed into a non-forest pixel with five temporal trajectories.
- Unstable change: A pixel that underwent irregular transformations from forest to non-forest and vice-versa making the transformation pattern hard to track.

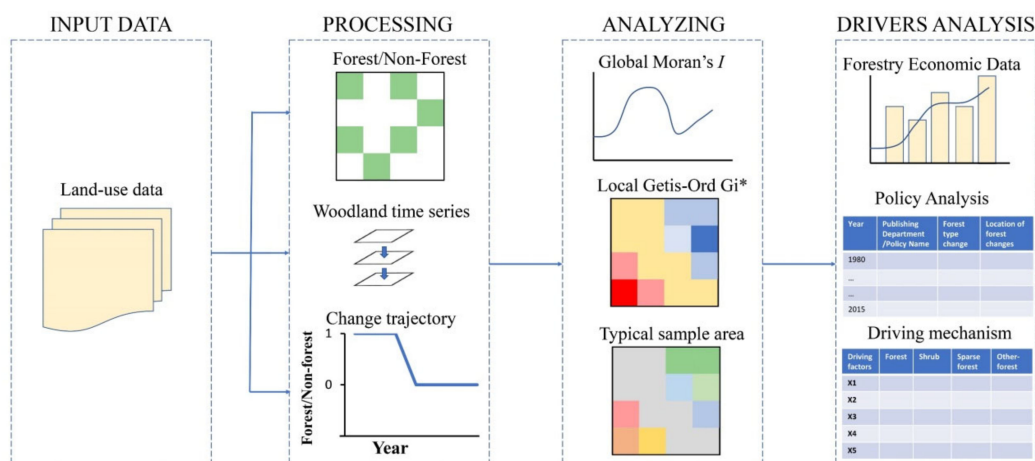


Figure 2. A graphical outline of the research framework.

The above-mentioned five change trajectories were summarized into three major categories namely: unchanged (Permanent forest and Permanent non-forest), stable (afforestation and deforestation) and unstable (the irregular change patterns).

To understand the role of policies on the forest change dynamics, the forest trajectories were linked to the forestry policies and economic factors adoption timelines bearing into consideration that there is a time lag between when the polices are adopted and when their impact would be reflected on the forest changes.

2.3.1. Forest Change Trajectories Dynamics

Following Zhou et al. (2011) [22] and Feng et al. (2014) [39], a temporal trajectory model was used to reveal patterns in the forest change dynamics. To keep tract of the change patterns, forested pixels were coded as 1 while non-forested pixels were coded as 0. The codes' change trajectories were tracked and analyzed within 5-timestep including 1980–1990, 1990–1995, 1995–2000, 2000–2005, and 2010–2015. Thus, a change trajectory of “1110000” as is illustrated in Figure 3 indicates a pixel that was a forested pixel in 1980, 1990, and 1995 but was a non-forested pixel in 2000, 2005, 2010 and 2015. In other words, the pixel underwent a conversion from forested pixel to non-forested pixel (deforestation) during 1980–2015.

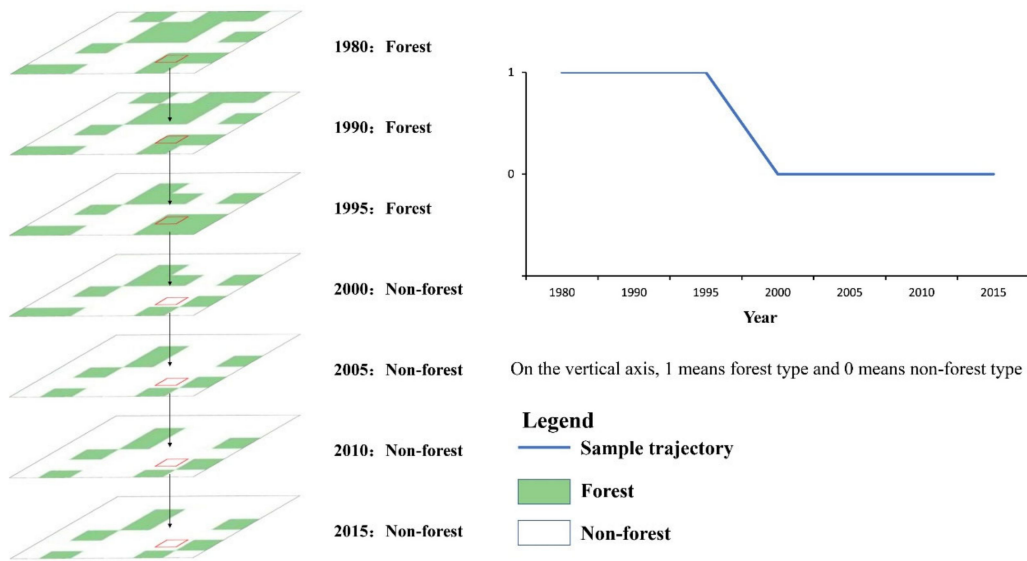


Figure 3. Example of forest temporal trajectory model.

2.3.2. Temporal and Spatial Cluster Analysis

The Global Moran's Index [40] was used to indicate the degree of forest's clustering in the timing of afforestation and deforestation. The global Moran's Index is given by:

$$I = \frac{n \sum_{i=1}^n \sum_{j=1}^n \omega_{i,j} Z_i Z_j}{S_0 \sum_{i=1}^n Z_i^2} \quad (1)$$

where Z_i is the deviation of an attribute for feature i from its mean ($x_i - \bar{X}$), $\omega_{i,j}$ is the spatial weight between feature i and j , n is the total number of features, and S_0 is the aggregate of all the spatial weights. S_0 is given by:

$$S_0 = \sum_{i=1}^n \sum_{j=1}^n \omega_{i,j} \quad (2)$$

To determine the degree into which the forested areas were cluttered spatially (gains and losses), a Local Getis-Ord G_i^* algorithm [41] was used. This method is robust in identifying areas with highly significant clustering (hot spot), which represents afforested areas, as well as those areas whose clustering was of low significance (cold spot), which represent deforested areas.

The Local Getis-Ord G_i^* algorithm is given by:

$$G_i^* = \frac{\sum_{j=1}^n \omega_{i,j} x_j - \bar{X} \sum_{j=1}^n \omega_{i,j}}{\sqrt{\frac{n \sum_{j=1}^n \omega_{i,j}^2 - (\sum_{j=1}^n \omega_{i,j})^2}{n-1}}} \quad \bar{X} = \frac{\sum_{j=1}^n x_j}{n} \quad S = \sqrt{\frac{\sum_{j=1}^n x_j^2}{n} - (\bar{x})^2} \quad (3)$$

where x_j is the attribute value of factor j and $\omega_{i,j}$ is the spatial weight between factor i and j , and n is the number of factors.

2.3.3. Driving Mechanisms Analysis

Forestry output value of various forest types (including the value of timber and other forest products) (X1), GDP per capita (X2), agricultural labors (X3), average altitude (X4) and average slope (X5) were correlated to closed-canopy forest (Y1), shrub (Y2), sparse forest (Y3), other-forest (Y4), total forest (Y5), afforestation (Y6) and deforestation

(Y7) to evaluate if there was a significant relationship, by employing a correlation analysis method within the SPSS software.

3. Results

3.1. The Spatial-Temporal Dynamics of Forest Types

Considering the whole study time frame (1980–2015), the coverage of the closed-canopy forest coverage which is the main forest type within GHKM decreased by 1477 km². However, slicing the study time frame into narrower time frames exposed the time bound trajectories of the change dynamics. For example, using the 1980–1995 timeframe, the analysis indicated that the closed-canopy forest area coverage increased by 1806 km². However, during 1995–2015, they experienced a negative trend and decreased by 3283 km². The magnitude of the negative change during 1995–2015 thus overweighed the positive experienced during 1980–1995 and hence the observed decrease reported when the full timeframe i.e., 1980–2015 is considered (Table 1). Interestingly, between 1980 and 2015, other-forest types increased by 2404 km². A breakdown of the temporal dynamics indicated that during 1980–1995 the other forests type was characterized by decreased trends in which 837 km² were lost while during the 1995–2010 they experienced an increasing trend in which 3291 km² were gained and hence the gain overweighed the loss. Narrowing the analysis to the forest types revealed that the area coverage of the sparse forest and the shrubs decreased by 806 and 165 km², respectively from 1980 to 2015.

Table 1. Temporal change of forest types in GHKM from 1980 to 2015 (km²). (“+” indicates increase, “−” indicates decrease).

	Closed-Canopy Forest	Shrub	Sparse Forest	Other-Forest	Total
1980–1990	+822	+73	−166	−93	+636
1990–1995	+984	−103	−112	−744	+25
1995–2000	−1187	−17	−31	+1211	−24
2000–2005	−356	−4	−50	+349	−61
2005–2010	−1105	−120	−392	+1731	+114
2010–2015	−635	+6	−55	−50	−734
1980–2015	−1477	−165	−806	+2404	−44

The GHKM-GBA region has witnessed rapid urban expansions since 1978; a factor that is highly attributed to the China’s reform and open policy. Within this region, forested areas have gradually been “swallowed” and dissolved by urban expansions. Illustrative of this is the reported decreased trends of forest cover in all major cities within GBA region except Hong Kong from 1980 to 2015. Macao, Dongguan and Shenzhen city all reported forest cover loss of greater than 10%, with Macao experiencing 15.79%, Dongguan 12.61% and Shenzhen 11.59% loss (Table 2). Within the WGR, EGR and NGR region (except Yunfu City), forest coverage increased at a slight rate. Among these regions, the largest forest area expansion was observed within the NGR region in which an increase of 461 km² was reported. Compared to the other regions, the highest increase rate (1.08%) of the forested areas was reported within the WGR.

Table 2. Forests' spatial dynamics in GHKM from 1980 to 2015.

Region	City	Percent Between Forest Area and the Total Area of Each City (%)						
		1980	1990	1995	2000	2005	2010	2015
GBA	Guangzhou	43.55	43.75	43.58	43.57	42.94	42.27	42.04
	Shenzhen	51.65	51.22	45.97	45.75	41.85	40.61	40.06
	Foshan	24.01	24.04	23.96	23.99	23.06	22.49	22.27
	Dongguan	35.08	35.12	31.56	31.40	24.89	22.92	22.47
	Huizhou	64.34	64.62	64.23	64.55	64.50	64.32	63.88
	Zhuhai	31.28	32.66	31.79	31.71	31.35	31.35	30.91
	Zhongshan	20.78	22.64	22.76	22.76	20.78	20.37	20.20
	Jiangmen	51.97	52.00	51.92	51.93	51.92	52.03	51.26
	Zhaoqing	75.66	75.89	75.82	75.91	75.81	75.89	75.25
	Hong Kong	58.31	58.31	57.78	57.78	58.31	58.41	58.41
	Macao	36.84	21.05	21.05	21.05	21.05	21.05	21.05
Total	55.76	55.99	55.48	55.56	54.89	54.62	54.13	
EGR	Shantou	24.15	24.38	26.29	24.48	24.62	24.71	24.66
	Shanwei	43.19	43.33	43.93	43.31	43.74	44.25	43.80
	Chaozhou	47.44	47.67	46.86	47.64	47.61	47.87	47.54
	Jieyang	45.73	45.96	45.84	46.03	46.18	46.34	45.88
	Total	42.23	42.44	42.69	42.46	42.66	42.94	42.57
NGR	Shaoguan	71.95	72.96	72.71	73.00	73.17	73.33	72.80
	Meizhou	74.93	75.89	75.97	75.91	76.08	76.39	75.98
	Heyuan	77.81	77.96	78.36	77.96	78.51	79.02	78.51
	Qingyuan	67.43	67.73	67.79	67.79	67.80	67.99	67.65
	Yunfu	70.07	70.42	70.37	70.37	70.33	70.34	69.93
Total	72.45	73.03	73.08	73.05	73.24	73.50	73.06	
WGR	Zhanjiang	33.40	33.67	35.25	35.30	36.16	36.15	36.02
	Yangjiang	58.55	58.48	58.86	58.78	58.96	59.13	58.78
	Maoming	59.55	59.59	59.65	59.51	59.66	59.74	59.55
	Total	49.13	49.23	49.96	49.91	50.35	50.42	50.21
GHKM	GHKM Cities	60.99	61.35	61.36	61.35	61.31	61.38	60.96

3.2. Forest Change Trajectories

Of the 50 temporal trajectories used to describe the forest dynamics during 1980–2015, 37 had an area of less than 100 km², which is less than 0.05% of the total study area (Table 3) and accounted for only 0.13% (Table 4). This implies that the change trends were mainly dictated by 13 main trajectories. The spatial distribution of the change types in the study area from 1980 to 2015 is graphically illustrated in a map in Figure 4. The non-forest areas were predominately high within the GBA region, and within the coastal areas of EGR and WGR. Since 1978, Shenzhen and Dongguan City has been a subject of rampant economic developments and urban expansion. Due to demand for space, these two cities have witnessed enormous conversion of forested areas into urban land. This explains the observed decreased in forest cover in Shenzhen and Dongguan, especially within the east bank of the Pearl River Estuary (Figure 4d). The NGR region is well known for state-owned forest farms. Thus, the scattered forest decrease observed within this region (Figure 4c) is attributed to the harvesting and planting of the artificial forests. Though the NGR region suffered scattered deforestation, it also benefitted afforestation (Figure 4b,c). Other regions in which afforestation was witnessed included the EGR (Figure 4e) and Leizhou Peninsula of WGR (Figure 4a).

Table 3. Proportions of 37 irregular change trajectories to the total area.

Trajectory	Area (km ²)	Proportion (%)	Trajectory	Area (km ²)	Proportion (%)
0010111	76	0.042	1110111	3	0.002
0011000	20	0.011	0000100	2	0.001
0100000	12	0.007	0000110	2	0.001
1100111	11	0.006	0011110	2	0.001
1110000	11	0.006	0101110	2	0.001
0000001	9	0.005	0111100	2	0.001
0111000	9	0.005	1010111	2	0.001
0111110	9	0.005	1011111	2	0.001
0001111	8	0.004	0001000	1	0.001
1111011	8	0.004	0001110	1	0.001
0101111	7	0.004	0010110	1	0.001
1101000	6	0.003	0101000	1	0.001
0010011	5	0.003	0101100	1	0.001
1101110	5	0.003	0110000	1	0.001
0000010	4	0.002	1000011	1	0.001
1101100	4	0.002	1000111	1	0.001
0011100	3	0.002	1100100	1	0.001
1010000	3	0.002	1111001	1	0.001
1100011	3	0.002			

Table 4. Reclassification of change trajectories to three types namely unchanged, stable and unstable.

Types	Trajectory	Number	Area (km ²)	Proportion (%)	
Unchanged type	Permanent Forest	1111111 1101111	2	105,828 249	59.073 0.139
	Permanent Non-forest	0000000 0010000	2	68,631 205	38.310 0.114
Stable change	Afforestation	0000011		332	0.185
		0000111	4	438	0.245
		0011111		453	0.253
		0111111		716	0.400
	Deforestation	1000000 1100000 1111000 1111100 1111110	5	114 445 553 226 718	0.064 0.248 0.309 0.126 0.401
Unstable change trajectory	0010111 0011000 0100000 1100111 0111000	37	240	0.134	

3.3. Spatio-Temporal Concentrations of Forest Dynamics

The degree of forest's clustering in the timing of forest dynamics in GHKM during 1990–2015 is graphically illustrated in Figure 5. Although the minimum Z value of forest dynamics in 2015 was 10.69, the probability of discrete state of forest dynamics was still less than 1%. During the 1990–2015, the agglomeration pattern increased from 1980 to 2005 and tended to weaken between 2005 and 2015. From 1995 to 2000, a reduction in forest change amplitude led to the decrease in the concentration degree and Z value. The forest change had the highest concentration and Global Moran's I reached a peak of 32.31 in 2005 (Figure 5).

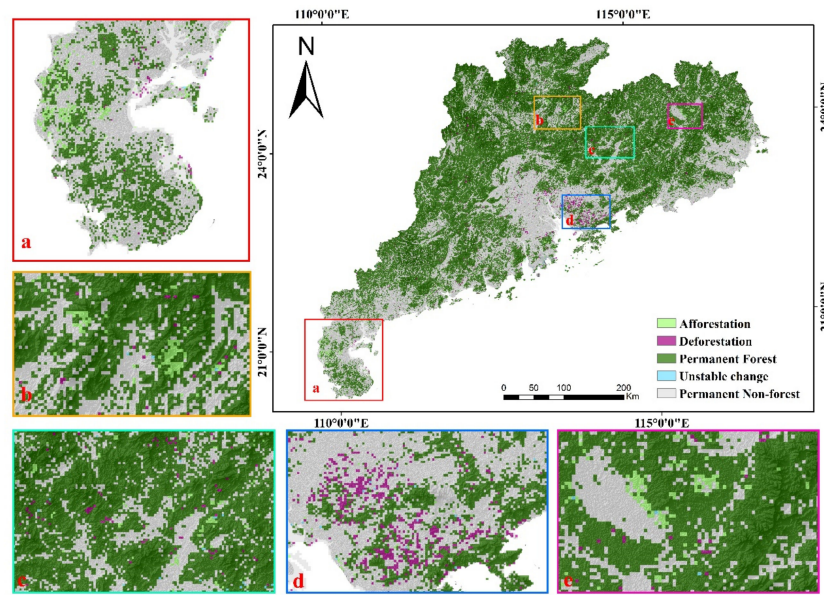


Figure 4. Five forest change trends in GHKM during 1980–2015: (a) obvious afforestation in Leizhou Peninsula; (b) obvious afforestation in NGR; (c) obvious artificial forest management and changes in NGR; (d) obvious deforestation in Shenzhen and Dongguan (GHKM-GBA); (e) obvious afforestation in EGR.

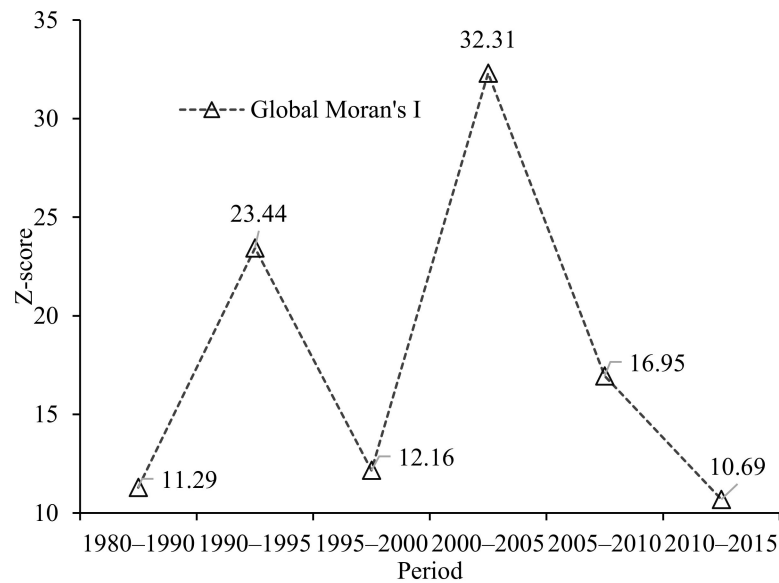


Figure 5. The degree of forest's clustering in the timing of forest dynamics within GHKM from 1980 to 2015.

The local Getis-Ord G_i^* revealed that forest hot spots that is areas that forest coverage was gained through afforestation were mainly distributed in Leizhou peninsula and mountainous regions of NGR and EGR. The cold spots that are areas which underwent deforestation were mainly concentrated in the GHKM-GBA (except Hong Kong and Macau), especially in Shenzhen and Dongguan City (Figure 6a). The deforestation reached its peak in Dongguan and Shenzhen during 2000–2005 and the east bank of the Pearl River Estuary was the most affected (Figure 6b). From 1980 to 1990, the NGR and EGR experienced a huge afforestation which was highly concentrated in Leizhou Peninsula that is located in Zhanjiang City of WGR during 1990–2005 (Figure 6c).

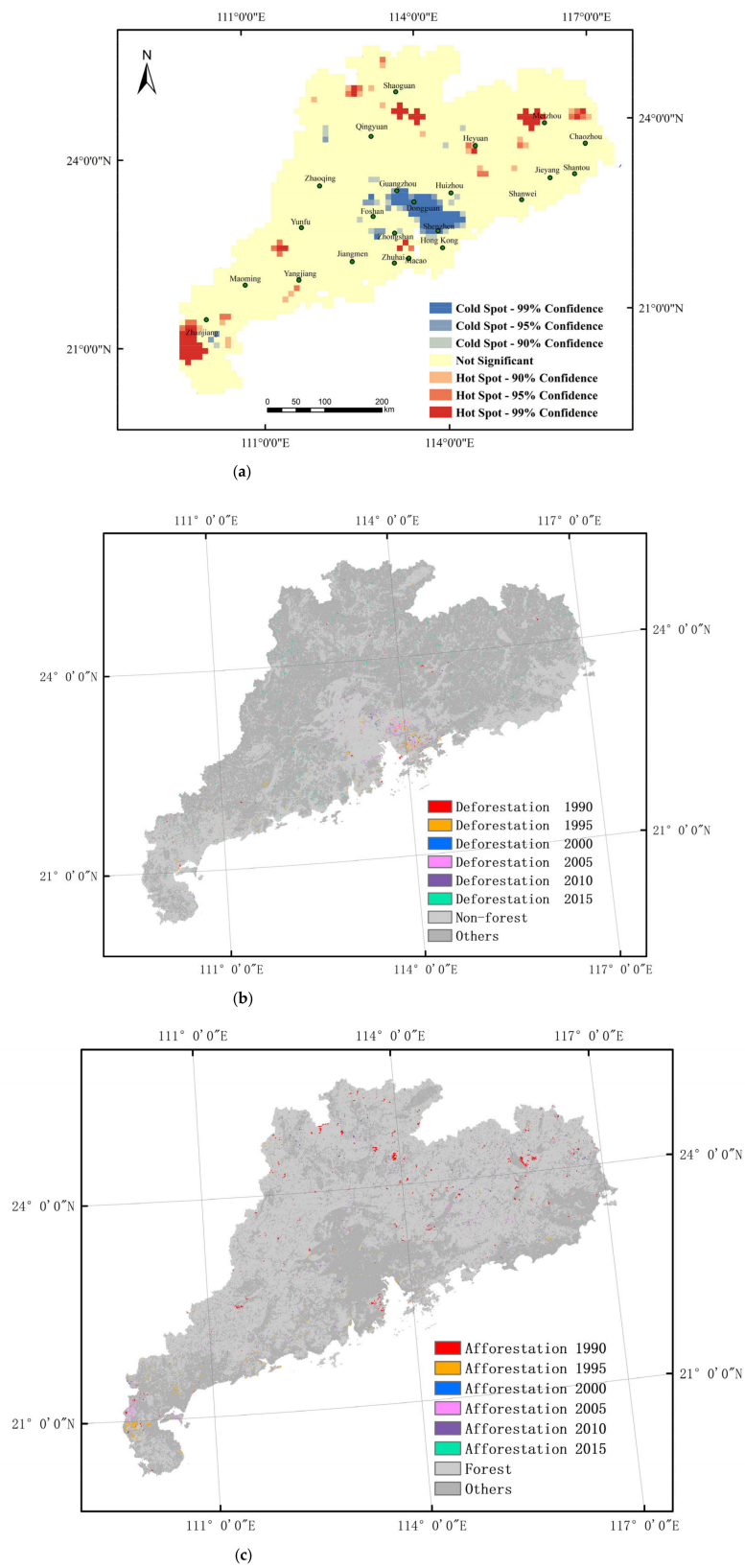


Figure 6. (a) Hot spot map of forest change; (b) spatial distribution of deforestation; (c) spatial distribution of afforestation.

3.4. Focus Plot Analysis

To highlight in detail the above changes, the analysis focused on three locations including the Leizhou Peninsula in WGR, the Wanlu lake in NGR and the Shenzhen City in GHKM-GBA.

- Leizhou Peninsula

This location is unique in that it is a huge artificial eucalyptus plantation zone. The plantations serve as an alternative source for short-cycle industrial timber. Artificial eucalyptus plantations revolution in this area started in mid-1980s in Guangdong as a response to meet the increased demand for wood and forest by-products [42]. Consequently, during 1990 to 1995, the Leizhou Peninsula witnessed increased forest cover gain as is reflected by the reported forest coverage gains of 2013 km² (Figure 7a). In addition, gains in forested areas in Leizhou Peninsula were reinforced by the adoption of the tropical orchards. Afforestation was highly concentrated within the central area of Leizhou Peninsula during 1990–2005 (Figure 7a).

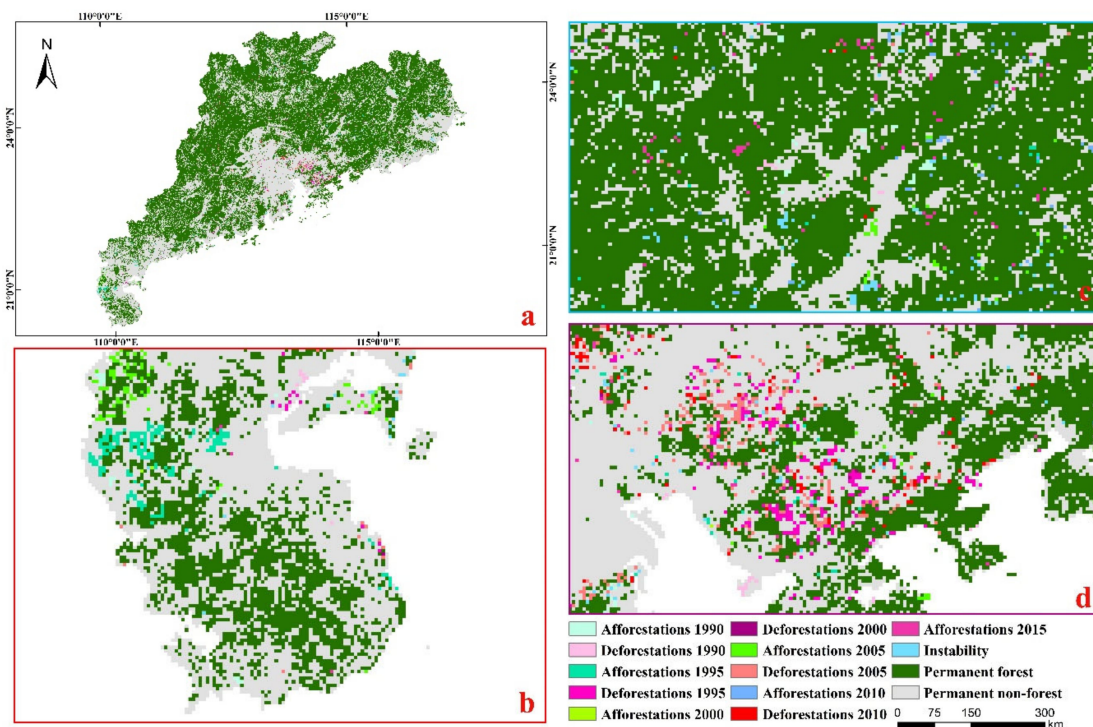


Figure 7. (a). Forest change trajectories in the study area during 1980–2015; the changes within the plots are highlighted in (b) the Leizhou Peninsula; (c) the Wanlu lake; (d) the Shenzhen City.

- Wanlu lake

This plot encompasses the mountainous region surrounding the Wanlu Lake (Figure 7b). This location is specifically unique with artificial mono-economic forests plantations for timber. The plantations are under a plantation-growth-logging-replantation management plan. The trajectories of the forest change dynamics in this region were characterized by the periodic change of forest. This was attributed to the temporal gaps in forest growth cycles under different management practices. Within the coastal area of Wanlu Lake, there was no significant difference between forest increases and decreases based on above-mentioned forest/non-forest maps during 1980–2015 and, hence, it was hard to track the dynamics of the change trajectories with clarity.

- Shenzhen city

The aftermaths of China's Economic Reform and Open policy were characterized by rapidly transformation of forested areas into urban land uses. Illustrative of this was the

forest cover change within the Shenzhen city in a massive forest cover loss of 214 km² during 1980–2015 at rate of 11.59% was reported (Figure 7c). In the late 20th century, Shenzhen had the fastest rate of forest loss but the rate gradually decreased after 2005. The forest cover loss rate within the Shenzhen decreased to 9.37% from 1990 to 2005. The remaining forest fragments were mainly concentrated in the eastern part of the city and hilly areas along the coast.

4. Discussion

4.1. Forest Change Dynamics Driven by Forestry Policies

The trajectories of forest change dynamics showed a response to the adoption of forest policies. Illustrative of this is the afforestation dynamics within the Guangdong city during 1980–1990 (Figure 8) whose timelines can be associated to the adoption of forest policies. For example, during this period, the National People’s Congress of China (NPCC) promulgated forest-related laws, following which the State Forestry Administration of China (SFAC) issued two forest-related policies in 1986 and in 1988. These two policies acted to reinforce the five forest policies issued by the Central Committee of the Communist Party of China (CCCPC) and the State Council of China (SCC) in 1980, 1981, 1982, 1984 and 1988. The impact of policies on the forest change dynamics was evident within Shaoguan, Qingyuan and Meizhou City in NGR, in which the forest coverage increased by of 636 km². Another impact from reinforcement of the policies on the forest change dynamics was the improvement of the forest structure as is indicated by increasing trends of the closed-canopy forest (822 km²), shrub (73 km²) compared to the reduced trend in which sparse forest and other-forest reduced by 166 km² and 93 km², respectively. However, the positive forest change trends in response to adoption and reinforcement of the forest policies were not spatially universal as some cities such as Shenzhen city experienced decreased forest cover. In 1991, the state law on soil and water conservation promulgated by NPCC was adopted. In 1994, SCC issued two forest protection acts, while in 1995, SFAC proposed the China’s forestry development plans. These two policies were aimed to reinforce sustainable forest conservation and management. There is always a time lag between policy inception and the manifestation of their impacts on the target. Though the initial policies were enacted in the 1980s, the trajectories of the forest dynamics which manifested as gains in forest area coverage reached the peak during 1990–1995. Illustrative of this was the closed-canopy forests, which increased their coverage by 984 km² during 1990–1995. This trajectory was, however, followed by a downward trajectory in which 1187 km² was lost during 1995–2000. The closed-canopy forest decline during 1990–2000 was a common in many parts of China, such as the Yangtze River Basin [43]. While the closed forest cover was decreasing during 1990–2000, the coverage of other-forest types increased by 1211 km² during 1995–2000. The increase in coverage of other forest types was linked to the adoption of the state agriculture laws which were promulgated by NPCC and enacted in 1993. The inception of the state agriculture laws influenced shifts in the market values and farmers opted for higher value-added forestry products. The result thereof was thus increased coverage of other forest types as is illustrated by the results. This observation resonates with observations by Wang and Zhang (2017) [44] on research on transition from a forestry policy-dominated status to a market-oriented status.

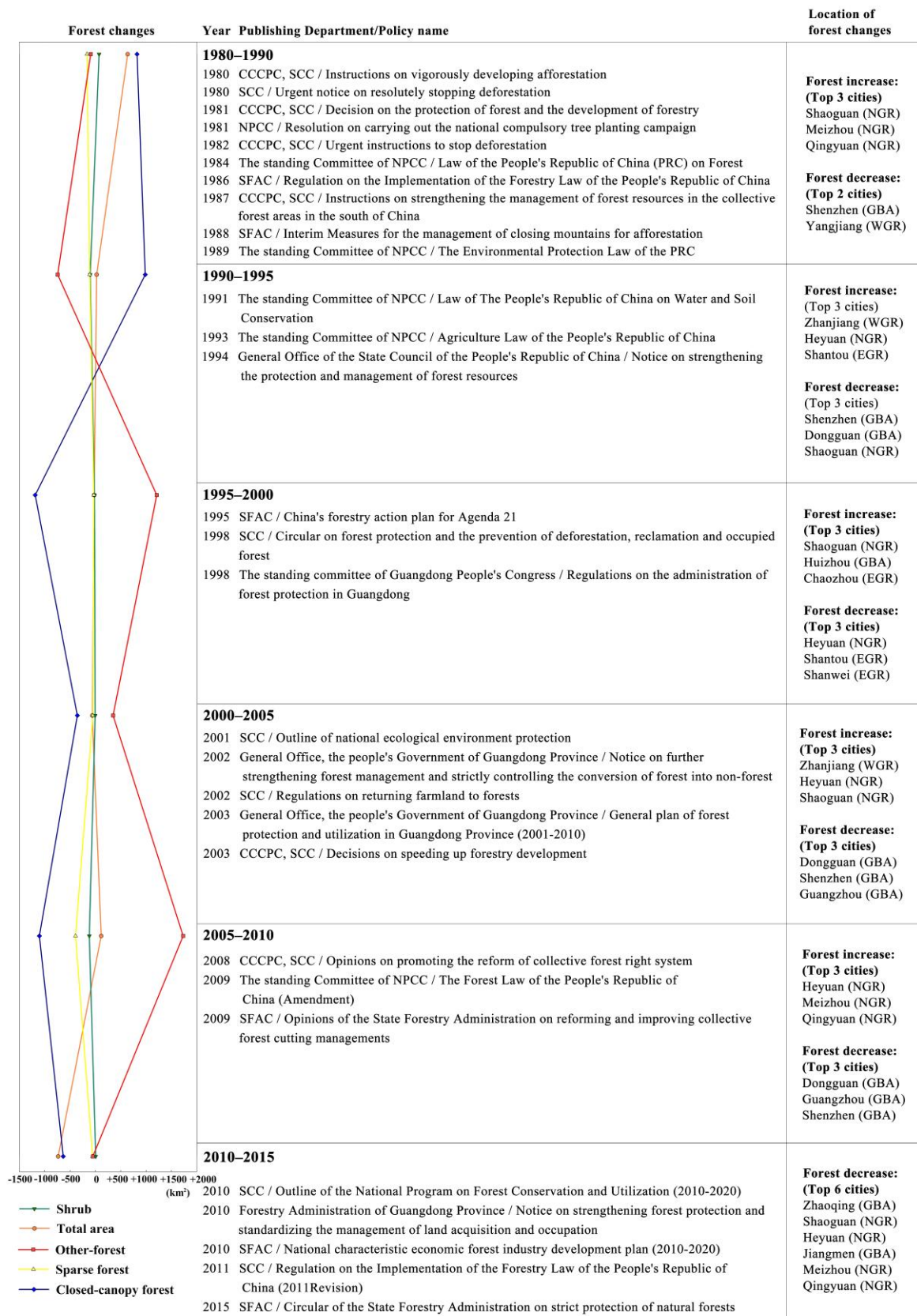


Figure 8. Forestry related policies and their impacts on forest dynamics.

The Yangtze River floods in 1998 and their effects thereof, alarmed decision and policy makers to promulgate forest laws and policies to which would catalyze, prioritize, and re-

inforce forest protection measures [45]. In response to the flood risk management and future prevention, SCC issued four policies in 1998, 2001, 2002 and 2003 whose mandate was to prohibit deforestation, promotion of ecological protection, conversion of farmland to forest and to accelerate the development and the implementation of sustainable forest management plans. Additionally, in 1998, the Guangdong province locally promulgated a local law to protect forest ecosystems. The effects of implementing these policies were reflected on the trajectories of forest dynamics between 2000 and 2005, and 2005 and 2010. Illustrative of this were the reduced rates at which the forest coverage declined. For example, the decline in closed-canopy forest during 2000–2005 was much lower (356 km²) compared to their decline rates (1187 km²) during 1995–2000. Moreover, the forest coverage in the mountainous regions (Shaoguan and Heyuan City) in the upper reaches of the Pearl River increased. This indicated that the forest policies and laws after the 1998 Yangtze River flood played a role in driving the trajectories of the forest change dynamics.

The policies and laws on the reform of collective forest right system issued between 2008 and 2009 (Figure 8) and the elimination of institutional obstacles inhibiting the development of forested areas greatly promoted the development of rural forested areas [44]. Illustrative of this was the observed increased trends of the areas covered by other-forests which gained coverage of 2080 km² between 2000 and 2010. The increase in the other-forest was particularly higher within the NGR and WGR region. This indicated that the forest management and developments were driven by the market values and hence the policies led to internal conversions of forests. The deforested areas were mainly dominant within the Shenzhen, Dongguan and Guangzhou City; all of which are within the GHKM-GBA region. Such forest loss is associated to the rapid urbanization because of increased economic development that was witnessed in this region.

During 2010–2015, forest area coverage decreased by 734 km². NGR region experienced the highest decline in which a total of 338 km² was lost, of which 236 km² was within areas with a slope of less than 15°. Within these areas, logging is legally permitted based on a series of laws and policies issued by SCC, SFAC and Guangdong Forestry Bureau. About 105 km² of the areas in which forest cover was lost and had slope of <15° were converted into built-up land while the rest of the areas were used for timber logging. The change trajectory of the forests during 2010–2015 was thus driven by activities permitted and regulated by laws and policies. This observation was also made by a taskforce which worked on the effective implementation of forestry laws and policies on forest protection and utilization [46]. Similarly, Viña et al. (2016) [12] also found that the GDP per capita showed a significant positive relationship with forest loss. Although the finding on the conversion of forest into non-forest was consistent with the conclusion from Hu and He (2010) [47], we found that forest utilization within NGR was reasonable and within the stipulated limits as outlined in policies and laws adopted during 2010–2015.

4.2. Economy-Oriented Forest Dynamics from 1990–2015

The forestry output value (X1) and GDP per capita (X2) had significant negative correlations to the sparse forest and the closed-canopy forest ($p < 0.05$) (Table 5). Similarly, the average altitude (X4) and average slope (X5) had a significant negative correlation to the closed-canopy forest ($p < 0.01$). On the other hand, the GDP per capita (X2), average altitude (X4) and average slope (X5) had a significantly positive correlation to the other-forest type ($p < 0.05$). This implied that the main force that drove the forest change dynamics was the physical factors such as the slope and altitude, and economic factors such as forestry output value and per capita GDP.

Table 5. The correlation coefficients of the driving factors of five land use types.

Driving Factors	Correlation Coefficient						
	Closed-Canopy Forest	Shrub	Sparse Forest	Other Forest	Total Forest	Afforestation	Deforestation
X1	−0.904 *	−0.851	−0.947 *	0.873	−0.823	−0.857	0.347
X2	−0.931 *	−0.896	−0.966 *	0.917 *	−0.770	−0.862	0.362
X3	0.481	0.734	0.743	−0.480	0.689	0.449	−0.748
X4	−0.966 **	−0.788	−0.866	0.961 *	−0.577	−0.812	0.079
X5	−0.977 **	−0.747	−0.849	0.955 *	0.623	−0.812	0.058

(* indicates the significance is less than 0.05, ** indicates the significance is less than 0.01).

On the other hand, agricultural population was not significantly correlated to forest types implying that their role in forest dynamics was insignificant (Table 5). Forestry output value and GDP per capita had a positive significant correlation to other-forest types. This was so because the other-forest types were mainly composed of artificial economic forests and orchards which have high economic benefits. The average slope $<12^\circ$ and altitude <300 m had a significant positive correlation to forest changes during 1980–2015. This is explained by the fact that at such a slope and altitude, the terrain limits the conversion of forests to other land uses. This is so because increased slope implies increased difficulty in land developments. This observation was consistent to the report by Wang et al. (2018) [48] which pointed out that afforestation was mainly concentrated in mountainous areas with a high slope.

4.3. Relevance of the Article to the Forest Resource Management and Future Outlooks

4.3.1. Relevance of the Article to the Forest Resource Management with GHKM Region

Analysis of the temporal trajectories of forest changes revealed forest dynamics within the GHKM region during 1980–2015 by capturing timelines of afforestation, deforestation, and irregular forest dynamics. Compared to the bi-temporal change detection, this method was more inclined to the real profiles of forest dynamics. The strength of using the temporal trajectory analysis is that the trajectory dynamics can be linked to the timelines of events and thus the force driving the trajectories can be determined. In this research, the temporal trajectories were used to capture the response of forest dynamics in relation to policy and economic factors during different periods. For example, forest change trajectories during 1980–1995 that revealed afforestation when tracked to the timelines of events were linked to forest' policy-oriented drivers. During 1995–2010, the forest dynamics were driven antagonistically by the forest policies and protection-oriented initiatives as well as economy-oriented forest usage. During 2010–2015, however, there was a shift in the forces driving the forest dynamics and the balance skewed to economy-oriented pressures, and hence the reported massive deforestation to pave space for urbanization and other economic developments. However, the deforestation was limited within regions with a slope below 15° , indicating that forestry policies still had the power to restrict economic activities within forested areas. Such insights provided new information on the role of forest policies and economic factors in forest management and protection. The results of this study reinforce the application of remotely sensed satellite observations in understating the synergistic and antagonism effects of policy-economic drivers of forest dynamics over time and space.

4.3.2. Research Future Outlooks

This study analyzed and elaborated the spatial and temporal dynamics of forest coverage and how they were influenced by forestry policies and economic factors. However, it was beyond the scope of this study to reveal the changes in bio-chemical variables of forest canopy, biomass, and the forest growth status all of which are important factors to holistically describe forest health changes. Therefore, we propose this as a future research opening in which future undertaking may consider the application of other forest health

indicators such as vegetation index, leaf area index (LAI) and other indicators to reflect the canopy features. In addition, we strongly propose inclusion of ecological functions and forest growth processes in the analysis which was also not within the scope of this study.

Accurate remote sensing observation windows are critical for precise detection of deforestation and afforestation processes. In this paper, a 5-year interval observation window could not adequately capture the afforestation and deforestation within areas of interest. For example, within the mountainous regions around the Wanlu Lake, the artificial forest planting cycle is generally less than 5 years. Therefore, it was hard for this study to capture the forest cover dynamics consequent of human activities within these areas using a timestep of 5 years. In the future, therefore, application of a denser remote sensing time-series to adequately capture the dynamics that occur within short temporal windows is recommended. Additionally, we will find a fitting quantitative method to analyze the role of synergies from different forestry policies on forest cover dynamics within various regions and cities in the study area.

5. Conclusions

The trajectories of forest change dynamics within GHKM region depicted a significant fluctuation of peaks (forest gain) and deeps (forest loss) in space and time during 1980–2015. While considering the whole study area, one gets the perception of forest cover decline. However, narrowing the analysis to focus on specific regions revealed the generalized perception of the whole study area masked the independent site-specific dynamics. Illustrative of this was the significant forest coverage gain witnessed within the NGR and the WGR region. This illustration demonstrates the specificities in the spatial domain. Similarly, the forest change trajectories highlighted time bound specificities. It is these time-bound change trajectories that allowed for tracking of the driving forces by linking the trajectories to the policies' adoption timelines. The trajectories reflected a process in which the drivers transformed from forestry policy orientation to economic factor orientation. During the early years of the study time frame i.e., during 1980–1990, the trajectory of the forest change dynamics assumed a peak implying gains in forest cover. The gains reflected the response of forest dynamics to adoption of policies which were later reinforced by issues that promoted ecological conservation and protection. The intermediate period during 1995–2010, the forest change trajectories reflected the response to the antagonistic effects of forest protection-oriented policies and the economy-oriented drivers. During the late period i.e., 2010–2015, the forest change trajectories assumed a deep implying a loss in forest cover. This loss reflected the response of the forest dynamics to the economy-oriented drivers. The weight of the forces driving the forest changes were skewed and shifted from policy-oriented to economic oriented factors. The impact of this shift was massive deforestation to meet the demand for space for urbanization and industrial developments. However, deforestation was mainly concentrated within the gentle slope plain areas where the policy allows deforestation at a slope of less than 15°. This shows that economy-oriented forest changes were still constrained by forestry policies. Through tracking and revealing forest change trajectories and linking them to the driving forces, this paper thus provides a line of evidence whose insights can inform platforms interested in developing precise, smart, and sustainable forest management plans within the GHKM region.

Author Contributions: Y.X.: Data curation, Formal analysis, Methodology, Validation, Writing—original draft, Writing—review & editing; Y.L.: Data curation, Formal analysis, Writing—original draft; Z.M.: Writing—review & editing; G.L.: Conceptualization, Funding acquisition, Methodology, Supervision, Writing—original draft, Writing—review & editing. All authors have read and agreed to the published version of the manuscript.

Funding: This work was supported by the Science and Technology Program of Guangdong Province, China (Grant number. 2018B020207002), National Natural Science Foundation of China (NSFC) (Grant number. 41901349), Foundation for Young Innovation Talents in Higher Education of Guangdong, China (Natural Science) (Grant number. 2018KQNCX054), and the Startup Foundation for Talented Scholars in South China Normal University (Grant number. 8S0472).

Institutional Review Board Statement: Not applicable.

Informed Consent Statement: Not applicable.

Data Availability Statement: The data presented in this study are openly available in [Data Center for Resources and Environmental Sciences, Chinese Academy of Sciences (RESDC), <http://www.resdc.cn/DOI/doi.aspx?DOIid=54>] at [DOI: 10.12078/2018070201], reference number [32].

Acknowledgments: We are grateful to the Data Center for Resources and Environmental Sciences, Chinese Academy of Sciences (RESDC) for sharing geographic gridded data with us. We are also grateful to two anonymous reviewers for their constructive comments and suggestions that helped to shape the final draft of this paper.

Conflicts of Interest: The authors declare that they have no known competing financial interests or personal relationships that could have appeared to influence the work reported in this paper.

References

1. Watson, J.E.M.; Evans, T.; Venter, O.; Williams, B.; Tulloch, A.; Stewart, C.; Thompson, I.; Ray, J.C.; Murray, K.; Salazar, A.; et al. The exceptional value of intact forest ecosystems. *Nat. Ecol. Evol.* **2018**, *2*, 599–610. [[CrossRef](#)]
2. Costanza, R.; d'Arge, R.; De Groot, R.; Farber, S.; Grasso, M.; Hannon, B.; Limburg, K.; Naeem, S.; O'Neill, R.V.; Paruelo, J.; et al. The value of the world's ecosystem services and natural capital. *Nature* **1997**, *387*, 253–260. [[CrossRef](#)]
3. Wu, G.; Xiao, H.; Zhao, J.; Shao, G.; Li, J. Forest ecosystem services of Changbai Mountain in China. *Sci. China* **2002**, *45*, 21–32. [[CrossRef](#)] [[PubMed](#)]
4. Foley, J.A.; DeFries, R.; Asner, G.P.; Barford, C.; Bonan, G.; Carpenter, S.R.; Chapin, F.S.; Coe, M.T.; Daily, G.C.; Gibbs, H.K.; et al. Global consequences of land use. *Science* **2005**, *309*, 570–574. [[CrossRef](#)] [[PubMed](#)]
5. Song, X.; Hanse, M.; Stehman, S.; Potapov, P.; Tyukavina, A.; Vermote, E.; Townshend, J. Global land change from 1982 to 2016. *Nature* **2018**, *560*, 639–643. [[CrossRef](#)]
6. Peñuelas, J.; Boada, M. A global change-induced biome shift in the Montseny Mountains (NE Spain). *Glob. Chang. Biol.* **2003**, *9*, 131–140. [[CrossRef](#)]
7. Root, T.L.; Price, J.T.; Hall, K.R.; Schneider, S.H.; Rosenzweig, C.; Pounds, J.A. Fingerprints of global warming on wild animals and plants. *Nature* **2003**, *421*, 57–60. [[CrossRef](#)]
8. Walther, G.R.; Post, E.; Convey, P.; Menzel, A.; Parmesan, C.; Beebee, T.J.C.; Fromentin, J.M.; Hoegh-Guldberg, O.; Bairlein, F. Ecological responses to recent climate change. *Nature* **2002**, *416*, 389–395. [[CrossRef](#)]
9. Chen, X.; Zhao, H.; Li, P.; Yin, Z. Remote sensing image-based analysis of the relationship between urban heat island and land use/cover changes. *Remote Sens. Environ.* **2006**, *104*, 133–146. [[CrossRef](#)]
10. Moulin, S.; Kergoat, L.; Viovy, N.; Dedieu, G. Global-scale assessment of vegetation phenology using NOAA/AVHRR satellite measurements. *J. Clim.* **1997**, *10*, 1154–1170. [[CrossRef](#)]
11. Salim, H.A.; Chen, X.; Gong, J. Analysis of Sudan vegetation dynamics using NOAA-AVHRR NDVI data from 1982–1993. *Asian J. Earth Sci.* **2010**, *3*, 20–34. [[CrossRef](#)]
12. Viña, A.; McConnell, W.J.; Yang, H.; Xu, Z.; Liu, J. Effects of conservation policy on China's forest recovery. *Sci. Adv.* **2016**, *2*, 1–8. [[CrossRef](#)] [[PubMed](#)]
13. Sánchez-Pinillos, M.; De Cáceres, M.; Ameztegui, A.; Coll, L. Temporal dimension of forest vulnerability to fire along successional trajectories. *J. Environ. Manag.* **2019**, *248*, 109301. [[CrossRef](#)] [[PubMed](#)]
14. Jin, S.; Sader, S.A. MODIS time-series imagery for forest disturbance detection and quantification of patch size effects. *Remote Sens. Environ.* **2005**, *99*, 462–470. [[CrossRef](#)]
15. Justice, C.O.; Vermote, E.; Townshend, J.R.G.; Defries, R.; Roy, D.P.; Hall, D.K.; Salomonson, V.V.; Privette, J.L.; Riggs, G.; Strahler, A.; et al. The moderate resolution imaging spectroradiometer (MODIS): Land remote sensing for global change research. *IEEE Trans. Geosci. Remote Sens.* **1998**, *36*, 1228–1249. [[CrossRef](#)]
16. Eresanya, E.O.; Daramola, M.T.; Durowoju, O.S.; Awoyele, P. Investigation of the changing patterns of the land use land cover over Osogbo and its environs. *R. Soc. Open Sci.* **2019**, *6*, 191021. [[CrossRef](#)]
17. Zhu, Z.; Woodcock, C.E. Continuous change detection and classification of land cover using all available Landsat data. *Remote Sens. Environ.* **2014**, *144*, 152–171. [[CrossRef](#)]
18. Coppin, P.; Jonckheere, I.; Nackaerts, K.; Muys, B.; Lambin, E. Digital change detection methods in ecosystem monitoring: A review. *Int. J. Remote Sens.* **2004**, *25*, 1565–1596. [[CrossRef](#)]
19. Zhou, Q.; Li, B.; Kurban, A. Trajectory analysis of land cover change in arid environment of China. *Int. J. Remote Sens.* **2008**, *29*, 1093–1107. [[CrossRef](#)]
20. Sierra, R. Dynamics and patterns of deforestation in the western Amazon: The Napo deforestation front, 1986–1996. *Appl. Geogr.* **2000**, *20*, 1–16. [[CrossRef](#)]
21. Mena, C.F. Trajectories of land-use and land-cover in the northern Ecuadorian Amazon: Temporal composition, spatial configuration, and probability of change. *Photogram. Eng. Remote Sens.* **2008**, *74*, 737–751. [[CrossRef](#)]

22. Zhou, Q.; Li, B.; Chen, Y. Remote sensing change detection and process analysis of long-term land use change and human impacts. *Ambio* **2011**, *40*, 807–818. [[CrossRef](#)] [[PubMed](#)]
23. Tang, X.; Bullock, E.L.; Olofsson, P.; Estel, S.; Woodcock, C.E. Near real-time monitoring of tropical forest disturbance: New algorithms and assessment framework. *Remote Sens. Environ.* **2019**, *224*, 202–218. [[CrossRef](#)]
24. Carmona, A.; Nahuelhual, L. Combining land transitions and trajectories in assessing forest cover change. *Appl. Geogr.* **2012**, *32*, 904–915. [[CrossRef](#)]
25. Liu, L.; Xu, X.; Liu, J.; Chen, X.; Ning, J. Impact of farmland change on production potential in China during 1990–2010. *J. Geogr. Sci.* **2015**, *25*, 19–34. [[CrossRef](#)]
26. Verbesselt, J.; Zeileis, A.; Herold, M. Near real-time disturbance detection using satellite image time series. *Remote Sens. Environ.* **2012**, *123*, 98–108. [[CrossRef](#)]
27. Huete, A.; Didan, K.; Miura, T.; Rodriguez, E.P.; Gao, X.; Ferreira, L.G. Overview of the radiometric and biophysical performance of the MODIS vegetation indices. *Remote Sens. Environ.* **2002**, *83*, 195–213. [[CrossRef](#)]
28. Souza, C.M.; Siqueira, J.V.; Sales, M.H.; Fonseca, A.V.; Ribeiro, J.G.; Numata, I.; Cochrane, M.A.; Barber, C.P.; Roberts, D.A.; Barlow, J. Ten-year Landsat classification of deforestation and forest degradation in the Brazilian amazon. *Remote Sens.* **2013**, *5*, 5493–5513. [[CrossRef](#)]
29. Escuin, S.; Navarro, R.; Fernández, P. Fire severity assessment by using NBR (Normalized Burn Ratio) and NDVI (Normalized Difference Vegetation Index) derived from Landsat TM/ETM Images. *Int. J. Remote Sens.* **2008**, *29*, 1053–1073. [[CrossRef](#)]
30. Xie, B. Status and optimization strategies of forestry development in Guangdong Province. *Agric. Sci. Technol. J.* **2017**, *7*, 196. (In Chinese)
31. Jian, Y.; Chen, Y.; Xie, Y.; Gong, J. Dynamic analysis of the spatial structure and evolution model of rural settlement in Guangdong Province from 1980 to 2015. *J. Ecol. Rural. Environ.* **2019**, *35*, 698–706. (In Chinese)
32. Xu, X.; Liu, J.; Zhang, S.; Li, R.; Yan, C.; Wu, S. China multi-period land use and land cover remote sensing monitoring data set (CNLUCC). Data Registration and Publishing System of Resource and Environmental Science Data Center, Chinese Academy of Sciences. 2018. Available online: <http://www.resdc.cn/DOI> (accessed on 18 January 2021). (In Chinese) [[CrossRef](#)]
33. Xu, X.; Liu, J.; Zhang, D.; Zeng, L. Spatial-temporal characteristics and driving forces of woodland resource change in Hainan Island in the last 15 years. *Resour. Sci.* **2004**, *2*, 100–107. (In Chinese)
34. Zhang, G.; Liu, J.; Zhang, Z. Spatial-temporal changes of cropland in China for the past 10 years based on remote sensing. *Acta Geogr. Sin.* **2013**, *3*, 323–332. (In Chinese)
35. Liu, J.; Zhang, Z.; Zhuang, D.; Wang, Y.; Zhou, W.; Zhang, S.; Li, R.; Jiang, N.; Wu, S. A study on the spatial-temporal dynamic changes of land-use and driving forces analyses of China in the 1990s. *Geogr. Res.* **2013**, *1*, 12. (In Chinese)
36. Liu, J.; Zhuang, Z.; Xu, X.; Kuang, W.; Zhou, W.; Zhuang, S.; Li, R.; Yan, C.; Yu, D.; Wu, S.; et al. Spatial Patterns and driving forces of land use change in China in the early 21st Century. *Acta Geogr. Sin.* **2009**, *64*, 1411–1420. (In Chinese) [[CrossRef](#)]
37. Liu, J.; Kuang, W.; Zhang, Z.; Xu, X.; Qin, Y.; Ning, J.; Zhou, W.; Zhang, S.; Li, R.; Yan, C.; et al. Spatiotemporal characteristics, patterns, and causes of land-use changes in China since the late 1980s. *J. Geogr. Sci.* **2014**, *24*, 195–210. [[CrossRef](#)]
38. Ning, J.; Liu, J.; Kuang, W.; Xu, X.; Zhang, S.; Yan, C.; Li, R.; Wu, S.; Hu, Y.; Du, G.; et al. Spatiotemporal patterns and characteristics of land-use change in China during 2010–2015. *J. Geogr. Sci.* **2018**, *28*, 547–562. [[CrossRef](#)]
39. Feng, H.; Liu, H.; Wu, L. Monitoring the Relationship between the land surface temperature change and urban growth in Beijing, China. *IEEE J. Sel. Top Appl. Earth Obs. Remote Sens.* **2014**, *7*, 4010–4019. [[CrossRef](#)]
40. Goodchild, M. *Spatial Autocorrelation (CATMOG 47)*; GeoBooks: Norwich, UK, 1986.
41. Getis, A.; Ord, K. The analysis of spatial association by use of distance statistics. *Geogr. Anal.* **1992**, *24*, 189–206. [[CrossRef](#)]
42. Qi, S. Eucalypt introduction and development status in China. *Guangxi For. Sci.* **2006**, *35*, 250–252. (In Chinese)
43. Wu, Y.; Zhang, Z.; Yu, S. Protecting forest resources and building a green shield: Thoughts from the 1998 Great Flood. *Prot. For. Sci. Technol.* **1999**, *1*, 44–45. (In Chinese)
44. Wang, M.; Zhang, H. A study of forestry policy evolution and development tendency in China after the reform and opening-up. *World For. Res.* **2017**, *30*, 7–11. (In Chinese)
45. Cui, H.; Wen, T.; Zheng, F.; Kong, X.; Mao, H. Discussion on policy evolvement of forestry construction since reform and opening up. *For. Econ.* **2009**, 38–43. (In Chinese) [[CrossRef](#)]
46. Gao, W. Temporal and Spatial Patterns of Human Activities and Effects of Soil Erosion on River Basin Scale: Case Study in the Water Source Area of the Middle Route of South-to-North Water Diversion Project. Ph.D. Thesis, Chinese Academy of Forestry, Beijing, China, 2017.
47. Hu, Y.; He, J. Evolution of forestry policy in China since 1949. *J. Beijing For. Univ. (Soc. Sci.)* **2010**, *11*, 21–27. (In Chinese)
48. Wang, H.; Yan, J.; Li, H. Forest transition and its explanation in contiguous destitute areas of China. *Acta Geogr. Sin.* **2018**, *73*, 1253–1267. (In Chinese)